

Ferromagnetic instability in a doped band gap semiconductor FeGa₃

K. Umeo,^{1,2,*} Y. Hadano,² S. Narazu,² T. Onimaru,² M. A. Avila,³ and T. Takabatake^{2,4}

¹*Cryogenics and Instrumental Analysis Division, N-BARD, Hiroshima University, Higashi-Hiroshima 739-8526, Japan*

²*Department of Quantum matter, AdSM, Hiroshima University, Higashi-Hiroshima 739-8530, Japan*

³*Centro de Ciências Naturais e Humanas, Universidade Federal do ABC, Santo André - SP, 09210-971, Brazil*

⁴*Institute for Advanced Materials Research, Hiroshima University, Higashi-Hiroshima 739-8530, Japan*

(Received 10 August 2012; published 31 October 2012)

We report the effects of electron doping on the ground state of a diamagnetic semiconductor FeGa₃ with a band gap of 0.5 eV. By means of electrical resistivity, magnetization, and specific heat measurements we have found that gradual substitution of Ge for Ga in FeGa_{3-y}Ge_y yields metallic conduction at a very small level of $y = 0.006$, then induces weak ferromagnetic (FM) order at $y = 0.13$ with a spontaneous moment of $0.1 \mu_B/\text{Fe}$ and a Curie temperature $T_C = 3.3$ K, which continues increasing to $T_C = 75$ K as doping reaches $y = 0.41$. The emergence of the FM state is accompanied by quantum critical behavior as observed in the specific heat, $C/T \propto -\ln T$, and in the magnetic susceptibility, $M/B \propto T^{-4/3}$. At $y = 0.09$, the specific heat divided by temperature C/T reaches a large value of $70 \text{ mJ K}^{-2} (\text{mol Fe})^{-1}$, twice as large as that reported for FeSi_{1-x}Ge_x with $x_c = 0.37$ and Fe_{1-x}Co_xSb₂ with $x_c = 0.3$ at their respective FM quantum critical points. The critical concentration $y_c = 0.13$ in FeGa_{3-y}Ge_y is quite small, despite the fact that its band gap is one order of magnitude larger than those in FeSi and FeSb₂. In contrast, no FM state emerges by substituting Co for Fe in Fe_{1-x}Co_xGa₃ in the whole range $0 \leq x \leq 1$, although both types of substitution should dope electrons into FeGa₃. The FM instability found in FeGa_{3-y}Ge_y indicates that strong electron correlations are induced by the disturbance of the Fe-3d-Ga-4p hybridization.

DOI: [10.1103/PhysRevB.86.144421](https://doi.org/10.1103/PhysRevB.86.144421)

PACS number(s): 71.30.+h, 72.80.Ga, 75.45.+j, 75.50.Pp

I. INTRODUCTION

Iron- and ruthenium-based semiconductors with band gaps of the order of 0.1 eV such as FeSi,¹⁻¹⁵ FeSb₂,¹⁶⁻²² FeGa₃,²³⁻³³ Fe₂VAl,³⁴ RuAl₂,³⁵ RuGa₃,²⁴ and RuIn₃,³⁶ have attracted considerable attention because of their unusual transport and magnetic behavior. These compounds have been intensively studied not only as candidate thermoelectric materials, but also from an academic interest in the mechanism of gap formation, which has been discussed in the context of strong correlations involving 3d or 4d bands, analogous to 4f bands in rare-earth-based Kondo semiconductors. In typical 4f Kondo semiconductors such as YbB₁₂ and Ce₃Pt₃Bi₄, a small gap of about 0.02 eV is formed by the hybridization of localized 4f states with the conduction bands.³⁷ Kondo semiconductors are distinguished from band-gap semiconductors by the following points: (i) The gap gradually disappears upon heating to a temperature which is lower than the gap energy, as observed in the temperature dependence of optical conductivity for FeSi and FeSb₂.^{3,6,18} (ii) The gap is strongly suppressed by substituting both the magnetic ion site and the ligand site at a low level. Thereby, the magnetization and electronic specific heat coefficient are largely enhanced. This enhancement is observed in Fe_{1-x}Co_xSi,^{2,11} FeSi_{1-x}Ge_x,¹⁰ Fe_{1-x}Co_xSb₂,^{20,21} and FeSb_{2-x}Sn_x.¹⁹ Recently, however, the above physical properties of FeSi and FeSb₂ have been explained by a minimum model of a covalent insulator within a single-site dynamical mean-field approximation.³⁸ Furthermore, the electronic structure of FeSi measured by photoemission experiments has no distinct features relevant to a Kondo picture, but is qualitatively explained within the band calculations by density functional theory without many-body effects.^{13,39,40} Therefore, it remains an issue whether FeSi and FeSb₂ are Kondo or usual semiconductors.

FeSi and FeSb₂ are nearly ferromagnetic semiconductors. In spite of the absence of magnetic order in both FeSi and CoSi, their mixed system Fe_{1-x}Co_xSi exhibits magnetic order in the range $0.05 < x < 0.8$.^{2,11} Small-angle neutron scattering experiments have revealed a helical spin magnetic structure with a long period of more than 300 \AA .² This magnetic structure is realized by the Dzyaloshinsky-Moriya interaction as found in B20 crystal structures without an inversion center. By applying magnetic fields, the helical structure easily transforms to the FM structure. Moreover, FeSi_{1-x}Ge_x ($x \geq 0.37$) and Fe_{1-x}Co_xSb₂ ($0.2 \leq x < 0.5$) also present the emergence of ferromagnetism.^{10,20,21} According to the local density approximation plus onsite Coulomb repulsion correction method, the semiconducting states in FeSi and FeSb₂ are close in energy to a FM and metallic state.^{5,41} Thereby, local Coulomb repulsions U of 3.7 and 2.6 eV were obtained for FeSi and FeSb₂, respectively.

FeGa₃ crystallizes into a tetragonal structure with space group $P4_2/mnm$. A narrow $d(\text{Fe})$ - $p(\text{Ga})$ hybridization band gap $E_g = 0.3$ to 0.5 eV is expected from the band structure calculations based on the density functional theory within the local density approximation.^{24,26} It is consistent with the observed gap of 0.25 to 0.47 eV (Refs. 25,27,28,32) for FeGa₃. This value is one order of magnitude larger than that in FeSi (Ref. 4) and FeSb₂,¹⁶ whose gaps are 0.08 and 0.02 eV, respectively. In FeGa₃, the absence of a significant impurity-induced density of states at the Fermi level E_F is indicated by an extremely small γ value of $0.03 \text{ mJ K}^{-2} \text{ mol}^{-1}$.²⁸ These facts suggest that correlation effects or the nature of the Kondo semiconductor in FeGa₃ are weaker than in FeSi and FeSb₂. This weak correlation effect in FeGa₃ manifests itself by the absence of a sharp peak at the valence band maximum just below E_F , as found in recent photoemission spectra.³² The magnetic susceptibility shows diamagnetism

below room temperature, and it increases exponentially with temperature above 500 K.^{27,28} Recently, it has been reported that Co substitution for Fe in $\text{Fe}_{1-x}\text{Co}_x\text{Ga}_3$ ($x = 0.05$) induces a crossover from the semiconducting state to a metallic state with weakly coupled local moments.²⁹

In order to investigate the mechanism of metallization and emergence of ferromagnetism induced by electron doping in FeGa_3 , we synthesized $3d$ -electron-doped $\text{Fe}_{1-x}\text{Co}_x\text{Ga}_3$ samples and $4p$ -electron-doped $\text{FeGa}_{3-y}\text{Ge}_y$ samples and measured the electrical resistivity ρ , specific heat C , and magnetization M . Our results demonstrate a doping-induced semiconductor-metal transition in both systems, but a weak FM state only in $\text{FeGa}_{3-y}\text{Ge}_y$ for $y \geq 0.13$. We discuss how doping effects in the FeGa_3 system differ from those in the FeSi and FeSb_2 systems.

II. EXPERIMENTAL DETAILS

Single crystals of $\text{Fe}_{1-x}\text{Co}_x\text{Ga}_3$ and $\text{FeGa}_{3-y}\text{Ge}_y$ were grown by a Ga self-flux method. Mixtures of high-purity elements in compositions $\text{Fe} : \text{Co} : \text{Ga} = 1 - X : X : 9$ ($0 \leq X \leq 1$) and $\text{Fe} : \text{Ga} : \text{Ge} = 1 : 8.5 : Y$ ($0.01 \leq Y \leq 3$) were sealed in evacuated silica ampoules. The ampoules were heated to 1100 °C and cooled over 150 hours to 500 °C, at which point the molten Ga flux was separated by decanting. The crystal compositions were determined by electron-probe microanalysis (EPMA) using a JEOL JXA-8200 analyzer. The effective Co doping levels in the crystals were found to roughly agree with the nominal composition X , whereas a maximum effective Ge doping of $y = 0.41$ results for an initial composition $Y = 3$. X-ray diffraction patterns of powdered samples confirmed that all alloys for $0 \leq x \leq 1$ and $y \leq 0.41$ crystallized in the FeGa_3 -type structure. No impurity phases in the single crystals were found by x-ray diffraction nor EPMA. The lattice parameters a and c , and the unit cell volume V are plotted in Fig. 1. The values of $a = 6.262$ (6.240) and $c = 6.556$ (6.439) Å of FeGa_3 (CoGa_3) are in good agreement with reported values.^{24,42} For $\text{Fe}_{1-x}\text{Co}_x\text{Ga}_3$, both a and c parameters decrease monotonically with increasing x from 0 to 1, following Vegard's law. $V(x = 1)$ is 2.5 % smaller

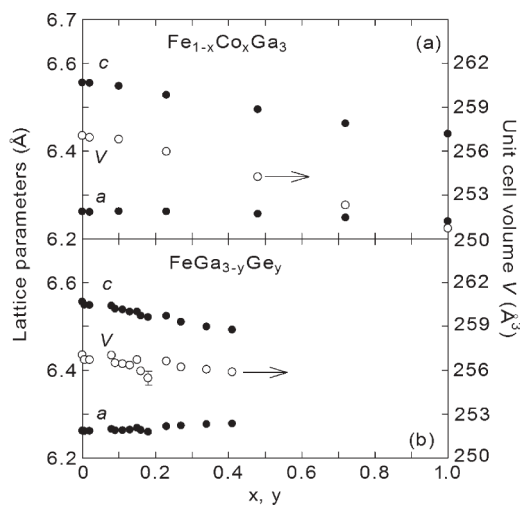


FIG. 1. Lattice parameters and unit cell volume of $\text{Fe}_{1-x}\text{Co}_x\text{Ga}_3$ (a) and $\text{FeGa}_{3-y}\text{Ge}_y$ (b) as a function of concentrations x and y .

than $V(x = 0)$. For $\text{FeGa}_{3-y}\text{Ge}_y$, the a value increases with increasing y , whereas the c value decreases. As a result, $V(y = 0.41)$ is only 1% smaller than $V(y = 0)$.

Resistivity measurements were performed on a home-built system using a standard four-probe ac method in the temperature range of 3–380 K provided by a Gifford-McMahon-type refrigerator. The magnetization M was measured under ambient pressure as well as applied pressures up to 2.21 GPa by using a superconducting quantum interference device (SQUID) magnetometer (Quantum Design MPMS) from 2 to 350 K and in magnetic fields up to 5 T. To measure M down to 0.35 K, we adopted a capacitive Faraday method using a high-resolution capacitive force-sensing device installed in a ^3He refrigerator.⁴³ The specific heat C from 0.3 to 300 K was measured by a relaxation method on a Quantum Design physical property measurement system (PPMS).

III. RESULTS

Figures 2(a) and 2(b) show the temperature dependence of ρ for $\text{Fe}_{1-x}\text{Co}_x\text{Ga}_3$ and $\text{FeGa}_{3-y}\text{Ge}_y$, respectively. For $\text{Fe}_{1-x}\text{Co}_x\text{Ga}_3$, the data are normalized by the ρ value at 380 K. The $\rho(T)$ data for $x = 0$ shown in the inset of Fig. 2(a) exhibit upturns in the temperature ranges of $T > 260$ K and $T < 50$ K, which are attributed to intrinsic response due to the band gap of 0.5 eV and extrinsic response due to impurity donors, respectively.²⁸ $\rho(T)/\rho_{380}$ for $x = 0.02$ increases with decreasing temperature in the entire temperature range. With increasing x , the upturn in $\rho(T)/\rho_{380}$ is suppressed and $\rho(T)/\rho_{380}$ for $x \geq 0.23$ shows metallic behavior. On the other hand, the substitution of Ge for Ga in $\text{FeGa}_{3-y}\text{Ge}_y$ at a very small level of $y = 0.006$ yields metallic conduction. It should be recalled that for $\text{Fe}_{1-x}\text{Co}_x\text{Si}$ and $\text{FeSi}_{1-x}\text{Ge}_x$,

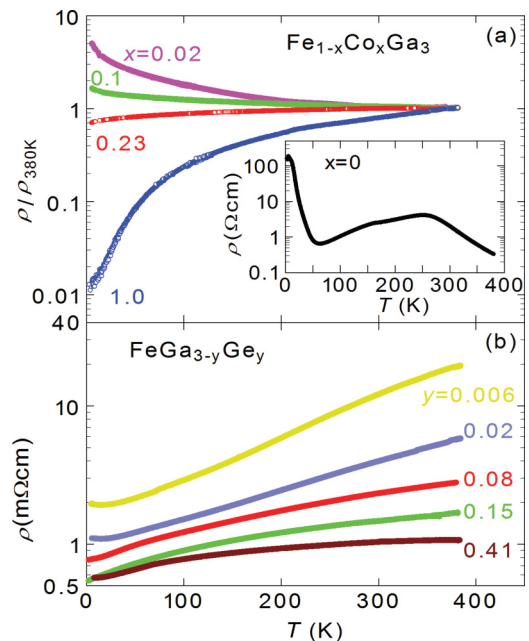


FIG. 2. (Color online) Temperature dependence of electrical resistivity ρ for $\text{Fe}_{1-x}\text{Co}_x\text{Ga}_3$ (a) and $\text{FeGa}_{3-y}\text{Ge}_y$ (b). The resistivity of $\text{Fe}_{1-x}\text{Co}_x\text{Ga}_3$ is normalized by the value at 380 K. The inset shows the resistivity for FeGa_3 ($x = 0$).²⁸

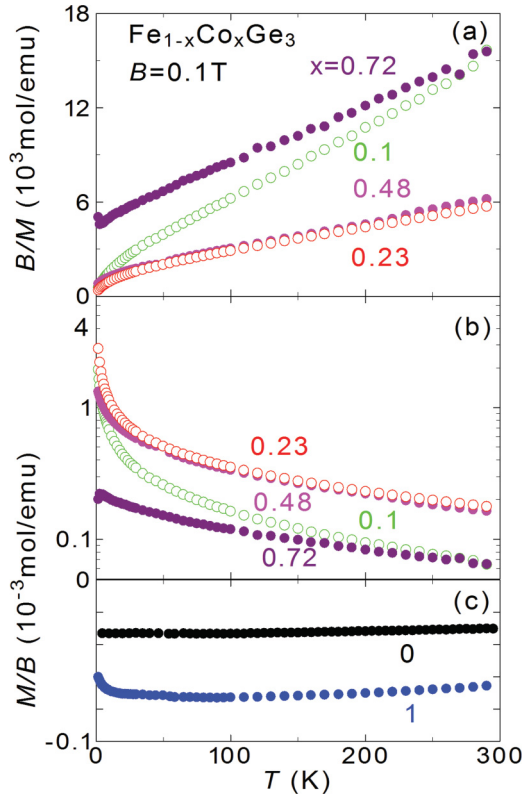


FIG. 3. (Color online) Temperature dependence of magnetic susceptibility M/B (b) and inverse magnetic susceptibility B/M (a) of $\text{Fe}_{1-x}\text{Co}_x\text{Ga}_3$

the semiconductor-metal transition occurs at the high levels of substitution $x = 0.6$ and 0.25 , respectively.^{10,11} Despite the fact that the band gap of 0.5 eV for FeGa_3 is one order of magnitude larger than that for FeSi , metallization occurs in $\text{FeGa}_{3-y}\text{Ge}_y$ at a much lower doping level, suggesting that Ge substitution in FeGa_3 introduces drastic changes in the electronic state.

The temperature dependence of the magnetic susceptibility M/B and its inverse B/M for $\text{Fe}_{1-x}\text{Co}_x\text{Ga}_3$ are displayed in Figs. 3(a), 3(b), and 3(c). The diamagnetic behavior for $x = 0$ and 1 suggests that the Fermi level lies in the energy gap. The $M/B(T)$ for $0.1 \leq x \leq 0.72$ shows Curie-Weiss paramagnetic behavior above 50 K. The negative value of the paramagnetic Curie temperature θ_p for $0.1 \leq x \leq 0.72$ implies that an antiferromagnetic interaction is dominant in this range.

On the other hand, a ferromagnetic (FM) order occurs in $\text{FeGa}_{3-y}\text{Ge}_y$ for $y \geq 0.13$. As shown in Fig. 4, a spontaneous magnetic moment saturation μ_s is observed in the magnetization curves $M(B)$ for $y \geq 0.13$ at 2 K, and μ_s increases with increasing y . However, μ_s is significantly smaller than that of Fe metal, $2.22 \mu_B/\text{Fe}$.⁴⁴ Furthermore, the M/B data as a function of temperature show a ferromagnetic behavior for $y \geq 0.13$ as shown in Fig. 5. This FM transition should be a bulk property because $C(T)$ has a clear anomaly at the T_C determined by the M/B data, as shown in the inset of Fig. 5.

Figure 6 shows the temperature dependence of the inverse magnetic susceptibility B/M of $\text{FeGa}_{3-y}\text{Ge}_y$. For $y \geq 0.08$, the B/M data follow the Curie-Weiss law. The value of θ_p for

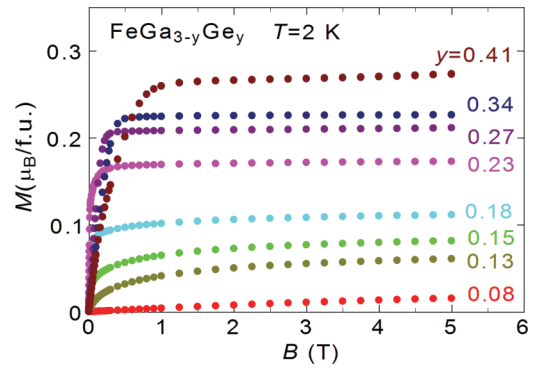


FIG. 4. (Color online) Isothermal magnetization curves of $\text{FeGa}_{3-y}\text{Ge}_y$ at 2 K.

$y \leq 0.09$ is negative, and changes to positive for $y \geq 0.13$. Both θ_p and the Curie temperature T_C as a function of y are displayed in the upper panel of the inset of Fig. 6. The temperature T_C was estimated as the temperature where the extrapolation of $M(T)^2$ becomes zero. The increase in both θ_p and T_C with increasing y indicates that the FM interaction is enhanced by Ge doping.

In order to study the nature of ferromagnetism in $\text{FeGa}_{3-y}\text{Ge}_y$ for $y \geq 0.13$, the pressure dependence of M was measured. Figure 7 shows the temperature dependence of M/B for $y = 0.34$ under various pressures P and the inset shows the pressure dependence of T_C . It is found that T_C decreases as $T_C \propto P^{3/4}$ which is predicted by the spin-fluctuation theory.⁴⁵ Furthermore, as shown in the lower panel of the inset of Fig. 6, the ratio of μ_{eff}/μ_s is as high as 4 to 10 . These findings suggest that $\text{FeGa}_{3-y}\text{Ge}_y$ for $y \geq 0.13$ is an itinerant weak ferromagnet.

The specific heat divided by temperature, C/T , as a function of T^2 for $\text{Fe}_{1-x}\text{Co}_x\text{Ga}_3$ and $\text{FeGa}_{3-y}\text{Ge}_y$ is shown in Fig. 8. The C/T data of $\text{FeGa}_{3-y}\text{Ge}_y$ for $0.05 \leq y \leq 0.15$ displays an upturn below 5 K. The electronic specific-heat coefficient γ was estimated by the extrapolation of the C/T data to $T = 0$. The variations of $T_C(y)$ for $\text{FeGa}_{3-y}\text{Ge}_y$ and γ (x and y) for $\text{Fe}_{1-x}\text{Co}_x\text{Ga}_3$ and $\text{FeGa}_{3-y}\text{Ge}_y$ are shown in Figs. 9(a) and 9(b). It is worth noting that $\gamma(y)$ exhibits a sharp peak of $70 \text{ mJ K}^{-2} \text{ mol}^{-1}$ at $y = 0.09$ near the critical

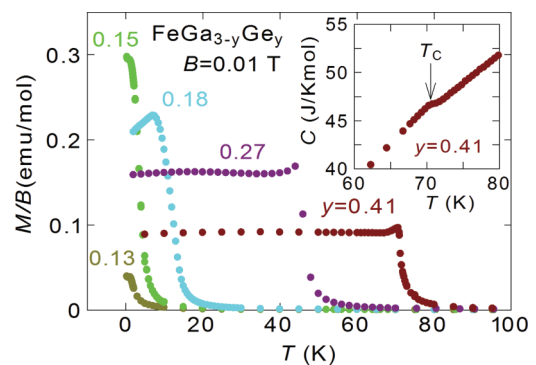


FIG. 5. (Color online) Temperature dependence of magnetic susceptibility M/B of $\text{FeGa}_{3-y}\text{Ge}_y$ for $y \geq 0.13$ where ferromagnetic transitions are observed. The inset shows the specific heat of $\text{FeGa}_{3-y}\text{Ge}_y$ for $y = 0.41$ near T_C .

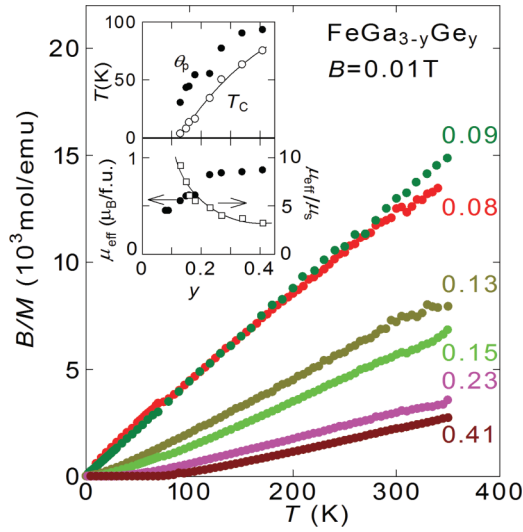


FIG. 6. (Color online) Temperature dependence of the inverse magnetic susceptibility B/M of $\text{FeGa}_{3-y}\text{Ge}_y$. The upper and lower panels of the inset show the paramagnetic Curie temperature θ_p and ferromagnetic transition temperature T_C , and effective magnetic moments μ_{eff} and the Rhodes-Wohlfarth value μ_{eff}/μ_s , respectively, as a function of y .

concentration $y_c = 0.13$ where the ground state changes from a nonmagnetic state to a FM state, clearly contrasting with the almost flat behavior in $\gamma(x)$ for $\text{Fe}_{1-x}\text{Co}_x\text{Ga}_3$. The value of $70 \text{ mJ K}^{-2} \text{ mol}^{-1}$ for $\gamma(y = 0.09)$ is enhanced by a factor of 2300 compared to $\gamma(y = 0) = 0.03 \text{ mJ K}^{-2} \text{ mol}^{-1}$.

The FM quantum critical behavior in C/T and M/B for $\text{FeGa}_{3-y}\text{Ge}_y$ ($y = 0.09$) are evidenced in the plots in Fig. 10. The specific heat and magnetic susceptibility for $y = 0.09$ follow the functional forms of $C/T \propto -\ln T$ and $M/B \propto T^{-4/3}$, which are predicted by the self-consistent renormalization (SCR) theory for FM spin fluctuations in three-dimensional systems.⁴⁶ These observations are consistent with the pressure dependence of $T_C \propto P^{3/4}$ in Fig. 7. On the other hand, as shown in Fig. 11, the T -linear dependence of $\rho(T)$ resistivity near the critical concentration of $y = 0.15$ is at variance with the $T^{5/3}$ dependence predicted by SCR theory. The $\rho(T)$ data for $y = 0.08$ at $T < 30 \text{ K}$ obeys $T^{1.9}$, which indicates the

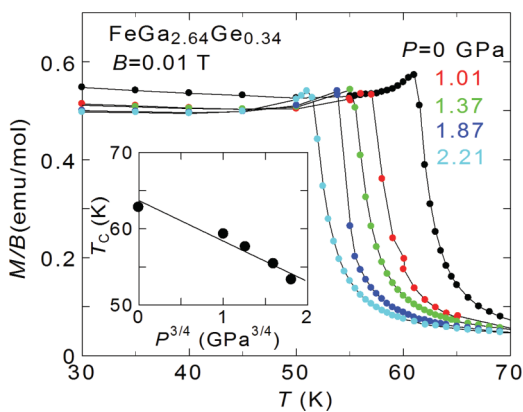


FIG. 7. (Color online) Temperature dependence of magnetic susceptibility M/B of $\text{FeGa}_{3-y}\text{Ge}_y$ for $y = 0.34$ under various pressures P . The inset shows T_C as a function of $P^{3/4}$.

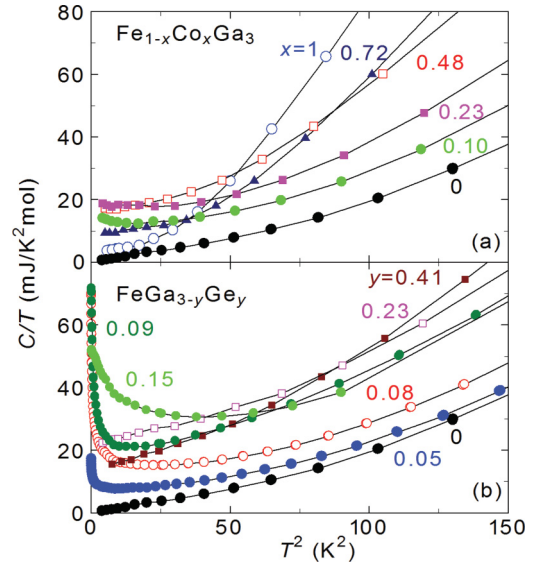


FIG. 8. (Color online) The specific heat divided by temperature C/T for $\text{Fe}_{1-x}\text{Co}_x\text{Ga}_3$ (a) and $\text{FeGa}_{3-y}\text{Ge}_y$ (b) as a function of T^2 .

recovery of the Fermi-liquid state. We will discuss the quantum critical behavior in $\text{FeGa}_{3-y}\text{Ge}_y$ in the next section.

IV. DISCUSSIONS

We now compare the doping effects on the electronic and magnetic states in $\text{Fe}_{1-x}\text{Co}_x\text{Ga}_3$ and $\text{FeGa}_{3-y}\text{Ge}_y$ with those in the FeSi and FeSb_2 systems. For $\text{Fe}_{1-x}\text{Co}_x\text{Ga}_3$, the semiconductor-metal transition occurs at $x = 0.23$, whereas no magnetically ordered state is induced in the whole range $0 \leq x \leq 1$. The gradual and weak change of $\gamma(x)$ for $\text{Fe}_{1-x}\text{Co}_x\text{Ga}_3$ suggests that the band structure changes in the rigid-band frame. A similar situation has been observed in $\text{Fe}_{1-x}\text{Co}_x\text{Si}$, which exhibits a helical magnetically ordered

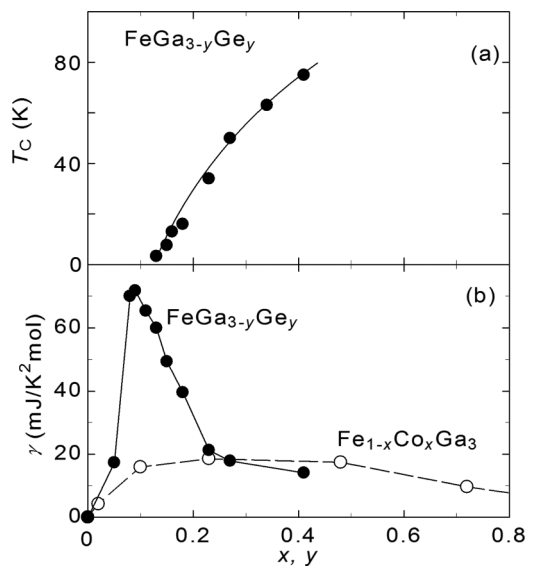


FIG. 9. Ferromagnetic transition temperature T_C (a) and electronic specific heat coefficient γ (b) for $\text{Fe}_{1-x}\text{Co}_x\text{Ga}_3$ and $\text{FeGa}_{3-y}\text{Ge}_y$ as a function of x and y .

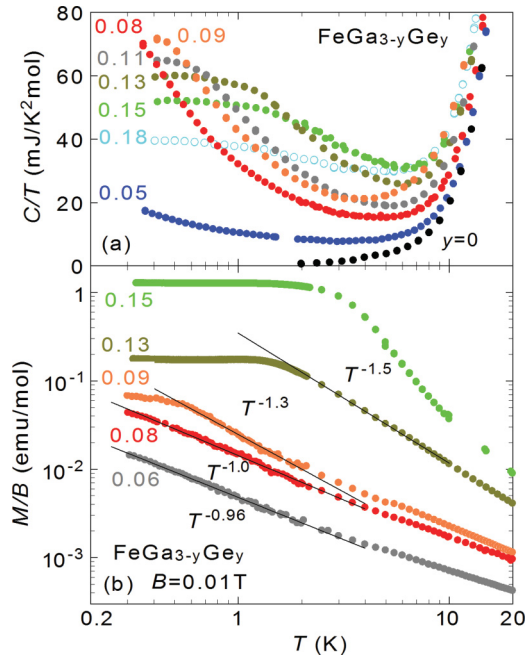


FIG. 10. (Color online) Logarithmic temperature dependence of C/T (a) and M/B (b) for $\text{FeGa}_{3-y}\text{Ge}_y$ near the FM instability.

state in the range $0.05 \leq x < 0.8$.¹¹ A photoemission study of $\text{Fe}_{1-x}\text{Co}_x\text{Si}$ revealed that the x dependence of the band structure near the Fermi level is described by the rigid-band model.⁴⁷ Therefore, the Stoner criterion can be applied to describe the magnetism of $\text{Fe}_{1-x}\text{Co}_x\text{Ga}_3$ and $\text{Fe}_{1-x}\text{Co}_x\text{Si}$. The criterion for the ferromagnetic state is given by the relation $UD(\varepsilon_F) \geq 1$, where U and $D(\varepsilon_F)$ are Coulomb repulsion and the density of states (DOS) at the Fermi level, respectively.⁴⁴ From a photoemission spectroscopy study of FeGa_3 , the magnitude of U was estimated to be 3 eV, which is comparable with 3.7 eV for FeSi .^{5,32} Therefore, the absence of a magnetically ordered state in $\text{Fe}_{1-x}\text{Co}_x\text{Ga}_3$ is a result of the fact that $D(\varepsilon_F)$ at the bottom of the conduction band for $\text{Fe}_{1-x}\text{Co}_x\text{Ga}_3$ is smaller than that for $\text{Fe}_{1-x}\text{Co}_x\text{Si}$.

On the other hand, for $\text{FeGa}_{3-y}\text{Ge}_y$, electron doping at the low level $y = 0.006$ already induces the semiconductor-metal transition. The Ga-site substitution disturbs the $3d-4p$ hybridization, which should lead to a dramatic change in

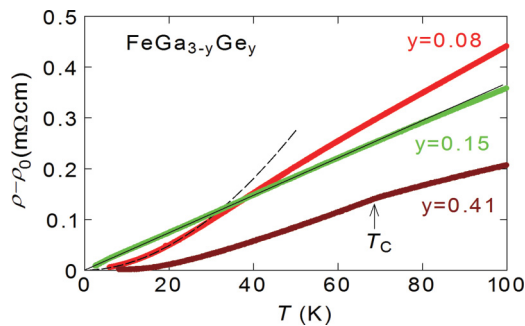


FIG. 11. (Color online) Temperature dependence of electrical resistivity ρ of $y = 0.08, 0.15$, and 0.41 for $\text{FeGa}_{3-y}\text{Ge}_y$. The $\rho(T)$ data for $y = 0.08$ and 0.15 were fit by $\rho - \rho_0 \propto T^{1.9}$ (broken line) and $\rho - \rho_0 \propto T$ (solid line), respectively.

the electronic state. Higher doping for $y \geq 0.13$ yields a FM order. The doping-induced FM state in the analogous system $\text{FeSi}_{1-x}\text{Ge}_x$ was explained by a mean-field slave-boson approach.¹⁰ Thereby, the key parameter driving the magnetic phases is the ratio between the Coulomb repulsion U and the hybridization of the localized-conduction electrons V . With increasing U/V , the paramagnetic ground state changes into an antiferromagnetic state and furthermore a FM state.⁴⁸ For $\text{FeGa}_{3-y}\text{Ge}_y$, the disturbance of the ligand Ga/Ge site may lead to the suppression of the $d-p$ hybridization V , whereas U in the Fe $3d$ shell would remain unchanged. Therefore, the Ga site substitution can yield the increase of U/V and thus induce a FM ground state. On the other hand, for $\text{Fe}_{1-x}\text{Co}_x\text{Ga}_3$, the Fermi level shifts maintaining a rigid band, whereby V does not change. Because U/V is almost constant against x , no magnetic order is realized. Very recently, the experimental data for resistivity, specific heat, and magnetization of $\text{FeSi}_{1-x}\text{Ge}_x$ have been explained by a minimal microscopic model.^{14,15} It is highly desirable to study whether this microscopic model is applicable for $\text{FeGa}_{3-y}\text{Ge}_y$.

Next, we focus on the FM quantum critical behavior (QCB) in $\text{FeGa}_{3-y}\text{Ge}_y$. Although ferromagnetic or antiferromagnetic QCB has been observed in many f -electron systems,⁴⁹ the FM QCB in d -transition-metal systems has been identified on a much smaller number of compounds, such as ZrZn_2 (Ref. 50) and $\text{Ni}_x\text{Pd}_{1-x}$.⁵¹ The FM QCB in these systems has been explained in terms of SCR theory.⁴⁶ For $\text{FeGa}_{3-y}\text{Ge}_y$, the experimental results of $C(T)$ and $M(T)/B$ near the critical concentration are consistent with the SCR theory of FM spin fluctuations, whereas the T -linear resistivity is at variance with the $T^{5/3}$ dependence predicted by this theory. Interestingly, $\text{Fe}_{0.7}\text{Co}_{0.3}\text{Si}$ shows T -linear resistivity under the critical pressure of 7 GPa,¹¹ whose origin of $\rho(T)$ is under debate. The resistivity is influenced by not only the spin fluctuations predicted by SCR theory but also the band structure and disorder in the crystal. Therefore, an elaborate theory considering the actual band structure and the inherent effect of disorder is needed to explain the observed resistivity. Nevertheless, the electron correlation effect in FeGa_3 is not significant compared with FeSi ,³² because of the absence of an impurity-induced density of states at the Fermi level indicated by the extremely small γ value of $0.03 \text{ mJ K}^{-2} \text{ mol}^{-1}$.²⁸ It is noteworthy that FeGa_3 with such a weak correlation effect, exhibits QCB near the critical point from the nonmagnetic state to the FM ground state. QCB may be induced by strong spin fluctuations due to the disturbance in the Fe- $3d$ -Ga- $4p$ hybridization. In order to clarify this point, neutron scattering studies on $\text{FeGa}_{3-y}\text{Ge}_y$ single crystals are highly desirable.

V. CONCLUSION

The effect of electron doping on the electronic and magnetic states of a diamagnetic semiconductor FeGa_3 with a rather large band gap of 0.5 eV has been studied using single crystalline samples of $\text{Fe}_{1-x}\text{Co}_x\text{Ga}_3$ and $\text{FeGa}_{3-y}\text{Ge}_y$. A semiconductor-metal transition in $\text{Fe}_{1-x}\text{Co}_x\text{Ga}_3$ occurs at $x = 0.23$, whereas no magnetic order is induced in the whole range $0 \leq x \leq 1$. These observations can be explained by the gradual change of the band structure in the rigid-band frame.

On the other hand, substitution of Ge for Ga in $\text{FeGa}_{3-y}\text{Ge}_y$ at a small value $y = 0.006$ yields metallic conduction, and further doping at $y = 0.13$ induces weak ferromagnetism. The γ value as a function of y exhibits a large peak of $70 \text{ mJ K}^{-2} (\text{mol Fe})^{-1}$ at $y = 0.09$. The critical concentration $y_c = 0.13$ for the ferromagnetism is rather small, in spite of the fact that the band gap of 0.5 eV is one order of magnitude larger than the gap sizes in FeSi and FeSb_2 . The FM quantum critical behaviors are manifested as $C/T \propto -\ln T$ and $M/B \propto T^{-4/3}$ near the critical concentration of $y_c = 0.13$ in $\text{FeGa}_{3-y}\text{Ge}_y$. This FM instability is attributed to strong electron correlations, which are induced by the disturbance in the $\text{Fe-}3d\text{-Ga-}4p$

hybridization by substituting Ge for Ga. Finally, we note that this system serves as a model system to investigate the FM instability in the simultaneous presence of disorder and electronic interaction, a problem that has been theoretically investigated.⁵²

ACKNOWLEDGMENTS

We thank F. Iga and for fruitful discussions. The magnetization and specific heat measurements were performed at N-BARD, Hiroshima University. This work was supported by the Scientific Research (A) (18204032) from MEXT, Japan.

*kumeo@sci.hiroshima-u.ac.jp

- ¹V. Jaccarino, G. K. Wertheim, J. H. Wernick, L. R. Walker, and S. Arajs, *Phys. Rev.* **160**, 476 (1967).
- ²J. Beille, J. Voiron, and M. Roth, *Solid State Commun.* **47**, 399 (1983).
- ³Z. Schlesinger, Z. Fisk, H.-T. Zhang, M. B. Maple, J. F. DiTusa, and G. Aeppli, *Phys. Rev. Lett.* **71**, 1748 (1993).
- ⁴D. Mandrus, J. L. Sarrao, A. Migliori, J. D. Thompson, and Z. Fisk, *Phys. Rev. B* **51**, 4763 (1995).
- ⁵V. I. Anisimov, S. Y. Ezhov, I. S. Elfimov, I. V. Solovyev, and T. M. Rice, *Phys. Rev. Lett.* **76**, 1735 (1996).
- ⁶S. Paschen, E. Felder, M. A. Chernikov, L. Degiorgi, H. Schwer, H. R. Ott, D. P. Young, J. L. Sarrao, and Z. Fisk, *Phys. Rev. B* **56**, 12916 (1997).
- ⁷B. Buschinger, C. Geibel, F. Steglich, D. Mandrus, D. Young, J. L. Sarrao, and Z. Fisk, *Physica B* **232**, 784 (1997); **230**, 784 (1997).
- ⁸V. I. Anisimov, R. Hlubina, M. A. Korotin, V. V. Mazurenko, T. M. Rice, A. O. Shorikov, and M. Sgrist, *Phys. Rev. Lett.* **89**, 257203 (2002).
- ⁹T. Saso and K. Urasaki, *J. Phys. Chem. Solids* **63**, 1475 (2002).
- ¹⁰S. Yeo, S. Nakatsuji, A. D. Bianchi, P. Schlottmann, Z. Fisk, L. Balicas, P. A. Stampe, and R. J. Kennedy, *Phys. Rev. Lett.* **91**, 046401 (2003).
- ¹¹Y. Onose, N. Takeshita, C. Terakura, H. Takagi, and Y. Tokura, *Phys. Rev. B* **72**, 224431 (2005).
- ¹²M. Arita, K. Shimada, Y. Takeda, M. Nakatake, H. Namatame, M. Taniguchi, H. Negishi, T. Oguchi, T. Saitoh, A. Fujimori, and T. Kanomata, *Phys. Rev. B* **77**, 205117 (2008).
- ¹³H. Yamaoka, M. Matsunami, R. Eguchi, Y. Ishida, N. Tsujii, Y. Takahashi, Y. Senba, H. Ohashi, and S. Shin, *Phys. Rev. B* **78**, 045125 (2008).
- ¹⁴D. Plencner and R. Hlubina, *Phys. Rev. B* **79**, 115106 (2009).
- ¹⁵J. Imriška and R. Hlubina, *Phys. Rev. B* **84**, 195144 (2011).
- ¹⁶C. Petrovic, J. W. Kim, S. L. Bud'ko, A. I. Goldman, P. C. Canfield, W. Choe, and G. J. Miller, *Phys. Rev. B* **67**, 155205 (2003).
- ¹⁷C. Petrovic, Y. Lee, T. Vogt, N. Dj. Lazarov, S. L. Bud'ko, and P. C. Canfield, *Phys. Rev. B* **72**, 045103 (2005).
- ¹⁸A. Perucchi, L. Degiorgi, R. Hu, C. Petrovic, and V. F. Mitrovic, *Eur. Phys. J. B* **54**, 175 (2006).
- ¹⁹A. Benti, G. K. H. Madsen, S. Johnsen, and B. B. Iversen, *Phys. Rev. B* **74**, 205105 (2006).
- ²⁰R. Hu, V. F. Mitrovic, and C. Petrovic, *Phys. Rev. B* **74**, 195130 (2006).

- ²¹R. Hu, R. P. Hermann, F. Grandjean, Y. Lee, J. B. Warren, V. F. Mitrovic, and C. Petrovic, *Phys. Rev. B* **76**, 224422 (2007).
- ²²A. Benti, S. Johnsen, G. K. H. Madsen, B. B. Iversen, and F. Steglich, *Europhys. Lett.* **80**, 17008 (2007).
- ²³C. Dasarthy and W. Hume-Rothery, *Proc. R. Soc. London, Ser. A* **286**, 141 (1965).
- ²⁴U. Häussermann, M. Boström, P. Viklund, Ö. Rapp, and T. Björnängen, *J. Solid State Chem.* **165**, 94 (2002).
- ²⁵Y. Amagai, A. Yamamoto, T. Iida, and Y. Takanashi, *J. Appl. Phys.* **96**, 5644 (2004).
- ²⁶Y. Imai and A. Watanabe, *Intermetallics* **14**, 722 (2006).
- ²⁷N. Tsujii, H. Yamaoka, M. Matsunami, R. Eguchi, Y. Ishida, Y. Senba, H. Ohashi, S. Shin, T. Furubayashi, H. Abe, and H. Kitazawa, *J. Phys. Soc. Jpn.* **77**, 024705 (2008).
- ²⁸Y. Hadano, S. Narazu, Marcos A. Avila, T. Onimaru, and T. Takabatake, *J. Phys. Soc. Jpn.* **78**, 013702 (2009).
- ²⁹E. M. Bittar, C. Capan, G. Seyfarth, P. G. Pagliuso, and Z. Fisk, *J. Phys.: Conf. Ser.* **200**, 012014 (2010).
- ³⁰Z. P. Yin and W. E. Pickett, *Phys. Rev. B* **82**, 155202 (2010).
- ³¹N. Haldolaarachchige, A. B. Karki, W. Adam Phelan, Y. M. Xiong, R. Jin, Julia Y. Chan, S. Stadler, and D. P. Young, *J. Appl. Phys.* **109**, 103712 (2011).
- ³²M. Arita, K. Shimada, Y. Utsumi, O. Morimoto, H. Sato, H. Namatame, M. Taniguchi, Y. Hadano, and T. Takabatake, *Phys. Rev. B* **83**, 245116 (2011).
- ³³V. G. Storchak, J. H. Brewer, R. L. Lichti, R. Hu, and C. Petrovic, *J. Phys.: Condens. Matter* **24**, 185601 (2012).
- ³⁴Y. Nishino, M. Kato, S. Asano, K. Soda, M. Hayasaki, and U. Mizutani, *Phys. Rev. Lett.* **79**, 1909 (1997).
- ³⁵D. N. Basov, F. S. Pierce, P. Volkov, S. J. Poon, and T. Timusk, *Phys. Rev. Lett.* **73**, 1865 (1994).
- ³⁶D. Bogdanov, K. Winzer, I. A. Nekrasov, and T. Pruschke, *J. Phys.: Condens. Matter* **19**, 232202 (2007).
- ³⁷T. Takabatake, F. Iga, T. Yoshino, Y. Echizen, K. Katoh, K. Kobayashi, M. Higa, N. Shimizu, Y. Bando, G. Nakamoto, H. Fujii, K. Izawa, T. Suzuki, T. Fujita, M. Sera, M. Hiroi, K. Maezawa, S. Mock, H. v. Löhneysen, A. Brückl, K. Neumaier, and K. Andres, *J. Magn. Magn. Mater.* **177–181**, 277 (1998).
- ³⁸J. Kuneš and V. I. Anisimov, *Phys. Rev. B* **78**, 033109 (2008).
- ³⁹D. Zur, D. Menzel, I. Jursic, J. Schoenes, L. Patthey, M. Neef, K. Doll, and G. Zwirgagl, *Phys. Rev. B* **75**, 165103 (2007).

- ⁴⁰M. Klein, D. Zur, D. Menzel, J. Schoenes, K. Doll, J. Roder, and F. Reinert, *Phys. Rev. Lett.* **101**, 046406 (2008).
- ⁴¹A. V. Lukoyanov, V. V. Mazurenko, V. I. Anisimov, M. Sigrist, and T. M. Rice, *Eur. Phys. J. B* **53**, 205 (2006).
- ⁴²P. Viklund, S. Lidin, P. Berastegui, and U. Häussermann, *J. Solid State Chem.* **165**, 100 (2002).
- ⁴³T. Sakakibara, H. Mitamura, T. Tayama, and H. Amitsuka, *Jpn. J. Appl. Phys.* **33**, 5067 (1994).
- ⁴⁴S. Blundell, in *Magnetism in Condensed Matter* (Oxford University Press, New York, 2001).
- ⁴⁵A. J. Millis, *Phys. Rev. B* **48**, 7183 (1993).
- ⁴⁶T. Moriya, in *Spin Fluctuation in Itinerant Electron Magnetism* (Springer-Verlag, Berlin, 1985).
- ⁴⁷J.-Y. Son, K. Okazaki, T. Mizokawa, A. Fujimori, T. Kanomata, and R. Note, *Phys. Rev. B* **68**, 134447 (2003).
- ⁴⁸V. Dorin and P. Schlottmann, *Phys. Rev. B* **46**, 10800 (1992).
- ⁴⁹G. R. Stewart, *Rev. Mod. Phys.* **73**, 797 (2001); K. Umeo, H. Kadomatsu, and T. Takabatake, *J. Phys.: Condens. Matter* **8**, 9743 (1996).
- ⁵⁰F. M. Grosche, C. Pfleiderer, G. J. McMullan, G. G. Lonzarich, and N. R. Bernhoeft, *Physica B* **206**, 20 (1995); **207**, 20 (1995).
- ⁵¹M. Nicklas, M. Brando, G. Knebel, F. Mayr, W. Trinkl, and A. Loidl, *Phys. Rev. Lett.* **82**, 4268 (1999).
- ⁵²P. B. Chakraborty, K. Byczuk, and D. Vollhardt, *Phys. Rev. B* **84**, 155123 (2011).